

Reprinted from

JOURNAL
OF THE
PHYSICAL
SOCIETY
OF
JAPAN



■ FULL PAPER

**One-Sample based Single-Valued Estimation of the Interface Profile
from Intersubband Integrated Absorption Intensity Data**

Dinh Nhu Thao, Nguyen Thanh Tien,
Huynh Ngoc Toan, and Doan Nhat Quang

J. Phys. Soc. Jpn. **85**, 074603 (2016)

One-Sample based Single-Valued Estimation of the Interface Profile from Intersubband Integrated Absorption Intensity Data

Dinh Nhu Thao^{1*}, Nguyen Thanh Tien², Huynh Ngoc Toan³, and Doan Nhat Quang⁴

¹College of Education, Hue University, 34 Le Loi Street, Hue City, Vietnam

²College of Natural Science, Can Tho University, 3-2 Road, Can Tho City, Vietnam

³Duy Tan University, K7/25 Quang Trung Street, Da Nang City, Vietnam

⁴Institute of Physics, Vietnamese Academy of Science and Technology, 10 Dao Tan Street, Hanoi, Vietnam

(Received April 29, 2016; accepted June 2, 2016; published online June 29, 2016)

We prove the integrated absorption intensity due to intersubband optical transition in a quantum well (QW) to be a function of the correlation length of the interface roughness profile and independent of the roughness amplitude. We then develop a novel way to perform single-valued estimation of the interface roughness profile of QW from experiments conducted merely on one sample. The new method that we propose in this paper would be replicable and more economical than the traditional counterparts, which usually require at least two samples.

1. Introduction

Roughness-related scatterings at low temperatures have been believed to be key scattering mechanisms in semiconductor nanostructures, e.g., a quantum well (QW). These scatterings potentially affect heterostructures (HSs) properties, which include optical spectra of intersubband transitions,¹⁻⁸ lateral transport,^{9,10} tunneling effect,¹¹ magnetic exchange bias,¹² and excitonic lineshape.¹³ Roughness was shown to give rise to strong scatterings in HSs in forms of surface roughness scattering,⁹ misfit deformation potential,^{14,15} misfit piezoelectric field in strained HSs,¹⁵ and polarization surface roughness scattering in polar HSs.¹⁰ Hence, roughness-related scatterings are critical factors in characterizing nanostructures.

The roughness is defined by its distribution in the in-plane and described by a roughness profile. This profile is specified by two parameters: roughness amplitude Δ and correlation length Λ . While the former parameter is the average height of roughness in the quantization direction, the latter is the size of a region in the in-plane, where the roughness at different points are correlated. Within the phenomenological model, the roughness profile is normally written as follows:

$$\langle |\Delta_{\mathbf{q}}|^2 \rangle = \pi(\Delta\Lambda)^2 F_R(q\Lambda), \quad (1)$$

where the roughness form factor $F_R(q\Lambda)$ depends solely on Λ , and is of certain shape, e.g., Gaussian,⁹ power-law,¹⁴ and exponential.¹⁶ Δ serves as a scaling factor, so fixing only the strength of the scattering, while Λ appears in both the scaling combination $\Delta\Lambda$ and the roughness form factor $F_R(q\Lambda)$, so fixing both the strength and the angular distribution of the scattering.

In order to perform theoretical analysis of the roughness-related effects^{1-7,9,10,13-15,17,18} one must include some roughness profile (Δ , Λ) as input parameters. It is very important to have Δ and Λ individually in order to test the validity of the interface roughness model and the key scattering mechanisms adopted in the theory. Thus, the single-valued estimation of roughness parameters has been an important issue over last decades, both theoretically and practically. A roughness profile of an open system, such as a surface QW, could be experimentally determined by a direct measurement of the roughness sizes (Δ and Λ) using atomic force microscopy. In

order to obtain the roughness profile of an interface QW, which is buried between two material layers, one can apply a measurement by cross-sectional scanning tunneling microscopy (XSTM).¹⁹ A number of theoretical studies have been developed to carry out the single-valued estimation of the two roughness parameters by fitting them simultaneously to different sets of data such as, absorption linewidth and mobility together.⁵

Recently, we introduced an experiment⁸ that executed a single-valued estimation of the correlation length by using data of the linewidth ratio only. Until then, we found no precedent studies that were able to separately evaluate Δ and Λ by fitting those parameters to the optical data. However, in this experiment, one should perform a measurement with two various samples that are assumed to possess the same roughness profile, which includes roughness amplitude and correlation length. This assumption is crucial yet and not feasible in actual experiment since variation of structure parameters of a system usually implies a modification of its roughness profile.²⁰ Fortunately, this shortcoming could be overcome by conducting suitable one-sample based experiments.

In this paper we report how we use the integrated absorption intensity due to intersubband optical absorption to build one kind of such one-sample based experiments. The integrated absorption intensity is a function of the correlation length and independent of the roughness amplitude. Since the integrated absorption intensity could be measured just using one sample (QW), single-valued estimation based on one sample of its correlation length would be performed using the integrated absorption intensity. In other words, we propose a measurement of the integrated absorption intensity on one sample for a reliable single-valued estimation of the correlation length.

2. Intersubband Optical Absorption

2.1 Microscopic theory of intersubband absorption

Let us consider the case when only the ground subband is occupied by electrons and the light energy is close to the energy separation between two lowest subbands: $\hbar\omega \sim E_{21} = E_2 - E_1$. The absorption of light polarized in the growth (z) direction is proportional to the real part of the dynamical conductivity.²¹ This was derived by a micro-

scopic theory of Ando.^{22,23} For single particle excitation, this reads as:

$$\text{Re } \sigma_{zz}(\omega) = \frac{e^2 f_{21}}{2m_z} \int dE \frac{m^*}{\pi \hbar} f(E) \frac{\Gamma(E)}{(\hbar\omega - E_{21})^2 + \Gamma^2(E)}, \quad (2)$$

where m_z and m^* are the out-of-plane and in-plane effective masses of the electron. f_{21} is the oscillator strength for the transition $E_1 \rightarrow E_2$ and $f(E)$ is the Fermi distribution function. $2\Gamma(E)$ represents the full width at half maximum (FWHM) of the Lorentzian lineshape with energy E , i.e., the energy broadening, given by

$$\Gamma(E) = \frac{1}{2} [\Gamma_{\text{intra}}(E) + \Gamma_{\text{inter}}(E)], \quad (3)$$

where the first term in square brackets arises from intrasubband processes, and second one from intersubband process.

The contributions to the energy broadening are supplied by⁴⁻⁶

$$\Gamma_{\text{intra}}(E) = \frac{m^*(\Delta\Lambda)^2}{\hbar^2} (F_{11} - F_{22})^2 \int_0^\pi d\theta e^{-q^2 \Lambda^2 / 4}, \quad (4)$$

$$\Gamma_{\text{inter}}(E) = \frac{m^*(\Delta\Lambda)^2}{\hbar^2} F_{12}^2 \int_0^\pi d\theta e^{-\tilde{q}^2 \Lambda^2 / 4}, \quad (5)$$

where q and \tilde{q} are the in-plane scattering vectors for the intrasubband and intersubband processes, and F_{mn} are the scattering form factors defined by the value of relevant wave functions at the potential barrier.⁸⁾

2.2 Characteristics of absorption spectrum

2.2.1 Peak of absorption

The absorption spectrum is peaked pronouncedly at the transition frequency $\omega = E_{21}/\hbar$ with a height given by

$$\sigma^p = \text{Re } \sigma_{zz}(E_{21}/\hbar) = \frac{e^2 f_{21}}{2m_z} \int dE \frac{m^*}{\pi \hbar} \frac{f(E)}{\Gamma(E)}. \quad (6)$$

The peak height is proportional to the inverse energy broadening $1/\Gamma(E)$, so to the inverse square of the scaling combination $(\Delta\Lambda)^{-2}$ by connecting Eqs. (3) to (5).

2.2.2 Linewidth

The lineshape described by Eq. (2) represents a superposition of Lorentzian lineshapes with different energies distributed following the Fermi function. Therefore, the spectral linewidth may be approximated by the average of their FWHMs with a weight $f(E)$:²³⁾ $\bar{\gamma} \approx 2\bar{\Gamma}$, where

$$\bar{\Gamma} = \int dE f(E) \Gamma(E) \left(\int dE f(E) \right)^{-1}. \quad (7)$$

In the opposite way to the peak height, the linewidth is proportional to the energy broadening $\Gamma(E)$, so to the square of the scaling combination $(\Delta\Lambda)^2$.

3. Estimation of the Correlation Length from Optical Data

Equations (6) and (7) show that characteristics of the absorption spectrum of a system, viz., peak height and linewidth, depend not only on the parameters of its structure (e.g., wellwidth) but also on those of the roughness profile such as $\sigma^p = \sigma^p(L; \Delta, \Lambda)$ and $\bar{\Gamma} = \bar{\Gamma}(L; \Delta, \Lambda)$. This dependence on the roughness profile enables experimental

estimation of the roughness parameters from optical data. Those experiments are classified into two main groups: two-sample and one-sample experiments.

3.1 Two-sample experiment

Two-sample experiment works with ratios of optical quantities such as ratio of linewidths or ratio of peak heights. The ratio of peak heights is denoted as

$$R_p = \frac{\sigma^p(L; \Delta, \Lambda)}{\sigma^p(L'; \Delta', \Lambda')} \quad (8)$$

and the ratio of linewidths is

$$R_w = \frac{\bar{\Gamma}(L; \Delta, \Lambda)}{\bar{\Gamma}(L'; \Delta', \Lambda')}. \quad (9)$$

The measurement of one of the above ratios claims the use of two samples. If the two samples are assumed to be various by some structure parameter such as wellwidth but have the same roughness profile, then the scaling combination $\Delta\Lambda$ drops out of the ratio in question. Hence, the ratio becomes a function of the correlation length only and is independent of the roughness amplitude. There exists, in this case, a possibility of a single-valued estimation of the correlation length from the ratio of linewidths or peak heights.⁸⁾

However, assuming two distinct samples to possess the same roughness profile is not feasible and non-controllable. Since the roughness profiles depend strictly on the system structure:²⁰⁾ $\Delta = \Delta(L)$, $\Lambda = \Lambda(L)$, so an inconsistency in values of those structure parameters can lead to significant variation between their corresponding roughness profiles. Therefore, experiments performed with only one sample might be a more reliable approach.

3.2 One-sample experiment

Following the above analysis, we now seek an one-sample based experiment that would help to perform a reliable single-valued estimation of the correlation length from the optical data. Previous studies⁴⁻⁸⁾ proposed that at low temperatures the intersubband optical absorption in semiconductor nanostructures is dominated by roughness-related scattering in absorption intensity, absorption energy and spectral linewidth. Thus, in principle, one can find two roughness sizes from the data of above quantities. We focus, in this case, on the integrated absorption intensity by some reasons as follows. The integrated absorption intensity in a QW is defined^{24,25)} as a product of its peak absorbance and spectral linewidth:

$$I(L, n_s; \Lambda) = \text{Re } \sigma_{zz}^p(L, n_s; \Delta, \Lambda) \times \bar{\gamma}(L, n_s; \Delta, \Lambda). \quad (10)$$

Besides, Eqs. (6) and (7) show that the scaling combination $\Delta\Lambda$ is eliminated from the right hand side of Eq. (10). In other words, the integrated absorption intensity becomes a function of the correlation length only, and does not depend on the roughness amplitude. Furthermore, as mentioned above, the integrated absorption intensity can be achieved using only one sample (QW). Therefore, using data of the integrated absorption intensity from one sample is sufficient to perform a single-valued estimation of the correlation length and so, of the interface roughness profile. Con-

sequently, we can find an approach to perform a reliable single-valued estimation of the correlation length from the optical data, and Eq. (10) is the heart of that theory.

3.3 Wave function

For a symmetric square QW,²⁶⁾ the wave functions are given as follows for the ground state:

$$\zeta_1(z) = C_1 \begin{cases} e^{\kappa_1(z+L/2)} \cos(k_1 L/2) & \text{if } z < -L/2 \\ \cos(k_1 z) & \text{if } |z| \leq L/2, \\ e^{-\kappa_1(z-L/2)} \cos(k_1 L/2) & \text{if } z > L/2 \end{cases} \quad (11)$$

where

$$C_1 = \frac{1}{\sqrt{L/2 + (V_0/\kappa_1 E_1) \cos^2(k_1 L/2)}} \quad (12)$$

with

$$\cos(k_1 L/2) - \frac{m_z^b \kappa_1}{m_z^c \kappa_1} \sin(k_1 L/2) = 0, \quad (13)$$

and for the first excited state:

$$\zeta_2(z) = C_2 \begin{cases} -e^{\kappa_2(z+L/2)} \sin(k_2 L/2) & \text{if } z < -L/2 \\ \sin(k_2 z) & \text{if } |z| \leq L/2, \\ e^{-\kappa_2(z-L/2)} \sin(k_2 L/2) & \text{if } z > L/2 \end{cases} \quad (14)$$

where

$$C_2 = \frac{1}{\sqrt{L/2 + (V_0/\kappa_2 E_2) \sin^2(k_2 L/2)}} \quad (15)$$

with

$$\cos(k_2 L/2) + \frac{m_z^c \kappa_2}{m_z^b \kappa_2} \sin(k_2 L/2) = 0, \quad (16)$$

where m_z^c and m_z^b are the out-of-plane effective mass of the electron in the channel and barrier, respectively. The wave number in the channel is $k_{1,2} = \sqrt{2m_z^c E_{1,2}}/\hbar$, and in the barrier $\kappa_{1,2} = \sqrt{2m_z^b (V_0 - E_{1,2})}/\hbar$.

3.4 Numerical results

In order to test our method, we deduce the interface roughness profile from intersubband optical absorption in the QW made of $\text{In}_{0.53}\text{Ga}_{0.47}\text{As}/\text{In}_{0.52}\text{Al}_{0.48}\text{As}$. In what follows we focus on the deduction of the roughness correlation length from optical data because the estimation of the roughness amplitude is straight afterwards.

The integrated absorption intensity due to a QW I is given approximately by the one due to the multiple QW I_M as follows:²⁴⁾

$$I \approx \frac{I_M}{W}, \quad (17)$$

where W is the number of single QWs forming the multiple QW, here $W = 70$. The dependence of the linewidth γ (in meV) and the multiple-QW integrated absorption intensity I_M (in meV) on the wellwidth L (in Å) could be found in Figs. 8 and 9 of Ref. 25, respectively. When $L = 35$: $I_M = 0.48$ and $\gamma = 32$; When $L = 100$: $I_M = 1.1$ and $\gamma = 13.7$. Structure parameters are found as follows:^{24,25)} barrier height: $V_0 = 500$ meV, the out-of-plane effective masses (in m_0): $m_z^c = 0.042$ and $m_z^b = 0.075$. We also attain the effective electron mass of the QW by averaging the effective electron masses in the channel (well) and barrier layers:

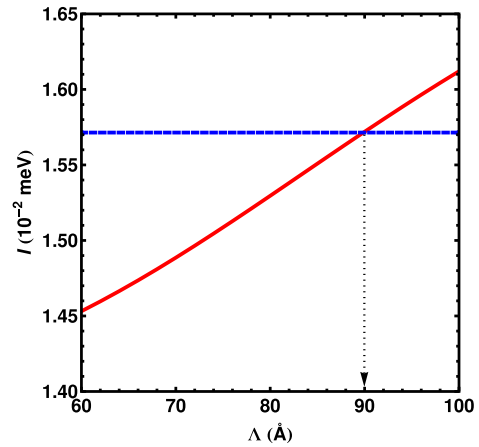


Fig. 1. (Color online) Integrated absorption intensity $I(L, n_s; \Lambda)$ for a QW, given by Eqs. (10), (6), (7), and plotted as a function of roughness correlation length Λ for a wellwidth $L = 100$ Å, $n_s = 0.1 \times 10^{13}$ cm⁻², and $I_M = 1.1$ meV.

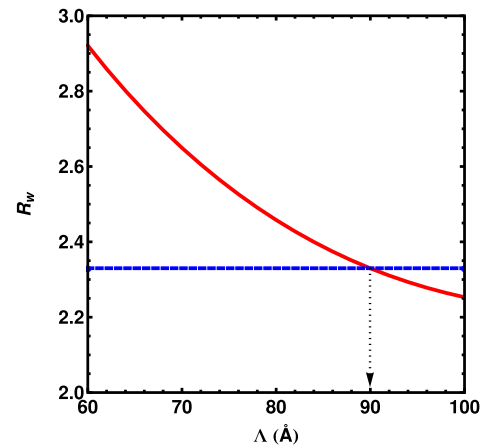


Fig. 2. (Color online) Linewidth ratio $R_W(L, n_s, L', n'_s; \Lambda)$ plotted as a function of correlation length Λ for various wellwidths: $\gamma(L = 35) = 32$, $\gamma(L' = 100) = 13.7$ with $n_s = 2.2 \times 10^{13}$ cm⁻² and $n'_s = 0.1 \times 10^{13}$ cm⁻², respectively.

$$m^* = \frac{m_z^c + m_z^b}{2} = 0.0585m_0. \quad (18)$$

In Fig. 1 the integrated absorption intensity for a QW $I(L, n_s; \Lambda)$ defined in Eq. (10) is plotted as a function of roughness correlation length Λ with QW parameters (wellwidth in Å, sheet electron density in 10^{13} cm⁻², the integrated absorption intensity in meV): $L = 100$, $n_s = 0.1$, and $I_M = 1.1$. The solid (red) curve and dashed (blue) line represents the calculation result and experiment data and the arrow points out the achieved roughness parameter, respectively. These indications also apply to other figures below. With $I \approx I_M/W = 0.0157$ meV we deduce $\Lambda = 90$ Å. The sample is a multiple QW formed of $W = 70$ QWs of $\text{In}_{0.53}\text{Ga}_{0.47}\text{As}/\text{In}_{0.52}\text{Al}_{0.48}\text{As}$.^{24,25)}

In order to compare our one-sample method to the two-sample counterpart that has been described recently,⁸⁾ in Fig. 2 we draw the linewidth ratio, $R_W(L, n_s, L', n'_s; \Lambda) = \gamma(L, n_s; \Delta, \Lambda)/\gamma(L', n'_s; \Delta, \Lambda)$ with the linewidth from Eq. (7), as a function of correlation length Λ for various wellwidths (linewidth in meV): $L = 35$, $\gamma = 32$, $n_s = 2.2$; $L' = 100$, $\gamma' = 13.7$, $n'_s = 0.1$. Then, with $R_W(\Lambda) = 2.33$, we also deduce

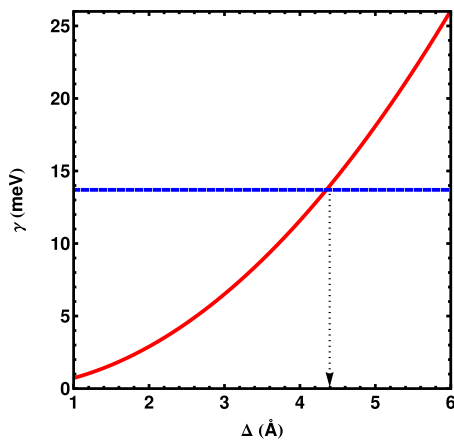


Fig. 3. (Color online) Linewidth $\gamma(\Delta)$ plotted as a function of roughness amplitude Δ with the fixed QW parameters: $L = 100 \text{ \AA}$, $n_s = 0.1 \times 10^{13} \text{ cm}^{-2}$, and with the correlation length taken from either Fig. 1 or 2 of $\Lambda = 90 \text{ \AA}$.

$\Lambda = 90 \text{ \AA}$. Our results confirm that, although the method that we proposed in this paper needs data from only one sample, it could compute the correlation length as efficiently, see Fig. 1, as does the two-sample precedent approach,⁸⁾ see Fig. 2.

To find the remaining roughness parameter, we may fit the roughness amplitude Δ to a linewidth,⁸⁾ or to some lifetime.²⁷⁾ For illustration, in Fig. 3, we fit the roughness amplitude Δ to the roughness-limited linewidth $\gamma(\Delta) = \gamma(L, n_s; \Delta; \Lambda)$ with the fixed QW parameters: $L = 100$, $n_s = 0.1 \times 10^{13} \text{ cm}^{-2}$, and the correlation length taken from Fig. 1 or 2 as: $\Lambda = 90 \text{ \AA}$. With $\gamma(\Delta) = 13.7 \text{ meV}$, we get $\Delta = 4.4 \text{ \AA}$. Both obtained values of two roughness sizes stay in their available ranges and coincide with the previous results.⁸⁾ In other words, the most prominent advantage of our new method lies in its ability to compute interface profile (Δ, Λ) by applying two-step fitting process on optical data of only one sample.

4. Summary

The inconsistency between interface profiles of two input samples could potentially violate the pivotal assumption of precedent two-sample method, weakening the reliability of the outcome computations. Therefore, we have proposed a novel approach to perform one-sample based single-valued estimation of the two sizes of interface roughness profile. This one-sample method processes optical data by a two-step fitting of (i) Λ to the integrated absorption intensity of a QW then (ii) Δ to some feature. We believe that our method could serve as a more reliable and economical alternative to the

traditional two-sample approach when the variance between the profiles of the two samples is significant.

Acknowledgment

This work was supported by the Vietnamese National Foundation for Science and Technology Development (NAFOSTED 103.02-2012.04).

*dnthao@dhsphue.edu.vn

- 1) K. L. Campman, H. Schmidt, A. Imamoglu, and A. C. Gossard, *Appl. Phys. Lett.* **69**, 2554 (1996).
- 2) J. B. Williams, M. S. Sherwin, K. D. Maranowski, and A. C. Gossard, *Phys. Rev. Lett.* **87**, 037401 (2001).
- 3) C. A. Ullrich and G. Vignale, *Phys. Rev. Lett.* **87**, 037402 (2001).
- 4) T. Unuma, T. Takahashi, T. Noda, M. Yoshita, H. Sakaki, M. Baba, and H. Akiyama, *Appl. Phys. Lett.* **78**, 3448 (2001).
- 5) T. Unuma, M. Yoshita, T. Noda, H. Sakaki, and H. Akiyama, *J. Appl. Phys.* **93**, 1586 (2003).
- 6) B. Mukhopadhyay and B. K. Basu, *Phys. Status Solidi B* **241**, 1859 (2004).
- 7) S. Tsujino, A. Borak, E. Müller, M. Scheinert, C. V. Falub, H. Sigg, D. Grützmacher, M. Giovannini, and J. Faist, *Appl. Phys. Lett.* **86**, 062113 (2005).
- 8) D. N. Quang, N. N. Dat, N. T. Tien, and D. N. Thao, *Appl. Phys. Lett.* **100**, 113103 (2012).
- 9) T. Ando, A. B. Fowler, and F. Stern, *Rev. Mod. Phys.* **54**, 437 (1982).
- 10) D. N. Quang, N. H. Tung, and N. T. Tien, *J. Appl. Phys.* **109**, 113711 (2011).
- 11) M. R. Brown, P. Rees, R. J. Cobley, K. S. Teng, S. Wilks, and A. Hughes, *J. Appl. Phys.* **102**, 113711 (2007).
- 12) M. Vafaei, S. Finizio, H. Deniz, D. Hesse, H. Zabel, G. Jakob, and M. Klui, *Appl. Phys. Lett.* **108**, 072401 (2016).
- 13) S. Glutsch and F. Bechstedt, *Superlattices Microstruct.* **15**, 5 (1994).
- 14) R. M. Feenstra and M. A. Lutz, *J. Appl. Phys.* **78**, 6091 (1995).
- 15) D. N. Quang, V. N. Tuoc, N. H. Tung, and T. D. Huan, *Phys. Rev. Lett.* **89**, 077601 (2002).
- 16) S. M. Goodnick, D. K. Ferry, C. W. Wilmsen, Z. Liliental, D. Fathy, and O. L. Krivanek, *Phys. Rev. B* **32**, 8171 (1985).
- 17) D. Zanato, S. Gokden, N. Balkan, B. K. Ridley, and W. J. Schaff, *Semicond. Sci. Technol.* **19**, 427 (2004).
- 18) D. R. Luhman, D. C. Tsui, L. N. Pfeiffer, and K. W. West, *Appl. Phys. Lett.* **91**, 072104 (2007).
- 19) I. Yamakawa, R. Oga, Y. Fujiwara, Y. Takeda, and A. Nakamura, *Appl. Phys. Lett.* **84**, 4436 (2004).
- 20) S. Arulkumaran, T. Egawa, H. Shikawa, and T. Jimbo, *J. Vac. Sci. Technol. B* **21**, 888 (2003).
- 21) M. Nakayama, *J. Phys. Soc. Jpn.* **39**, 265 (1975).
- 22) T. Ando, *J. Phys. Soc. Jpn.* **44**, 475 (1978).
- 23) T. Ando, *J. Phys. Soc. Jpn.* **54**, 2671 (1985).
- 24) H. Asai and Y. Kawamura, *Appl. Phys. Lett.* **56**, 1427 (1990).
- 25) H. Asai and Y. Kawamura, *Phys. Rev. B* **43**, 4748 (1991).
- 26) H. C. Liu, in *Quantum Well Infrared Photodetectors: Physics and Applications*, ed. H. Schneider and H. C. Liu (Springer, Berlin, 2007) Chap. 3, p. 13.
- 27) D. N. Quang, N. H. Tung, N. T. Hong, and T. T. Hai, *Appl. Phys. Lett.* **94**, 072106 (2009).